

HELICAL TWISTED EFFECT OF SPIRAL PIPE IN GENERATING SWIRL FLOW FOR COAL SLURRIES CONVEYANCE

Yanuar^{a*}, Kurniawan T. Waskito^a, Sealtial Mau^b, Winda Wulandari^b, Sri P. Sari^c

^aDepartment of Mechanical Engineering, University of Indonesia, Jakarta, 16424, Indonesia

^bGraduate Student Department of Mechanical Engineering, University of Indonesia, Jakarta, 16424, Indonesia

^cDepartment of Mechanical Engineering, Gunadarma University, Depok, 16424, Indonesia

Article history

Received

21 January 2017

Received in revised form

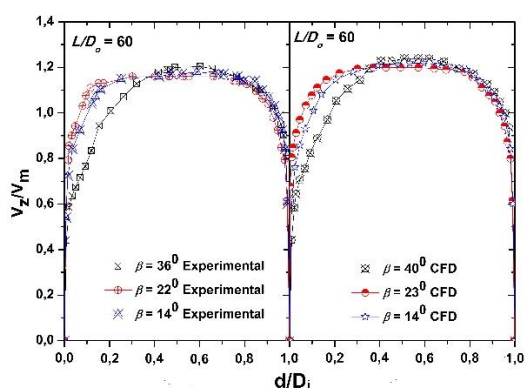
31 May 2017

Accepted

17 August 2017

*Corresponding author
yanuar@eng.ui.ac.id

Graphical abstract



Abstract

This paper proposes methods to reduce energy consumption for the transportation of coal slurries. Spiral pipe is one of the methods that can improve drag reduction at certain velocity as well as prevent decomposition at the pipe bottom and generate homogenous particles distribution. The objective is to investigate the influence of using spiral pipe to pressure drop and homogeneity of coal slurries. The pipe angles (β) are 14° , 23° , 40° and 56° , the pipe test loop is set up with entrance length 3000 mm. Pressure Transducer and pitot tube are used in the measurements. Percentage of the particle concentrations are varied by weight of 30 %, 40 % and 50 %. The helical angle gives significant effect to eliminate decomposition at the pipe bottom. At C_w 50 %, homogeneity of the slurries can reach around 96 % at helical angle 23° , It means the mixture between solid material and water more uniform, using circular pipe the homogeneity is only 74 %. Weight concentration of the solid particles and Reynolds number gives significant effect to the drag reduction. Flow of CW =50 % slurry at $Re \sim 5 \times 10^4$ through 23° spiral pipe can increase drag reduction by about 30%. Velocity profiles were obtained from numerical CFD simulation validated experimental results make clear the flow characteristics.

Keywords: Coal slurries, drag reduction, helical angle, homogeneity, spiral pipe

© 2017 Penerbit UTM Press. All rights reserved

1.0 INTRODUCTION

Coal is an important fuel for power plants. Its transportation in the form of slurry has received considerable attention since the successful construction of the Black Mesa Pipeline. In fact, one of the longest slurry pipelines is the ETSI coal pipeline, built in 1979. It spans a distance of 1670 km (1036 miles), uses a 965 mm (38 in) pipe, and transports 23 million metric tons/year (25 US tons/year). In Russia, the Siberian coal pipeline is 260 km (163 mi) long and transports 4 million tons of coal a year from Siberian

mines [1]. Spiral pipe gives significant as the solution in fluids that contained solid particles transport replace the conventional circular pipe that occurred sedimentation problem. It is possible to reduce sedimentation using circular pipe, but it needs high velocity in order to generate turbulent flow, of course it is not cost benefit because high velocity will produce high pressure drop, and consume more energy.

Leninger *et al.* [2] classified the types of coal transported as slurry power plant coal, coking coal, flotation tailings, hydrocoal or hydromechanically extracted coal. Hydromechanically extracted coal

(hydrocal) may be transported in a natural state, without grinding, over short distances. Particle sizes may range from 0–60 mm (0–2.4 in). The density of coal varies depending on the moisture content. An average specific gravity of 1.35 is often used in calculations.

Gas, liquid and multiphase fluids could be efficiently carried using pipeline transport system. Slurry is a type of multiphase fluid consisting of particles of solid and liquid. Characteristics of slurry is influenced by particle distribution, pipe size, particles size, particle concentration and liquid ratio, the level of turbulence, temperature and viscosity. In order to flow the multiphase fluid such as slurry, further studies are need to investigate the efficient methods due to the higher density of the fluids.

Energy saving in fluid transport system through pipelines keep on developing. Two methods were developed that are passive control and active control. Passive control method modifying the pipe surface to reduce energy consumption, meanwhile, active control modifying the working fluid to reduce friction factor caused by turbulence in the flow. Modifications were made to the working fluid by adding additives such as surfactants and polymers, even using micro bubble such as application in external flow by Yanuar *et al.* [3]. When the working fluid is dispersed, additives would reduce the friction factor on particular Reynolds number.

For the Multiphase flows, in general, there are three types of streams, namely; homogeneous, heterogeneous, and intermediate suspension. These flow types depend on the characteristics of the fluid. Mizue M *et al.* [4] investigated the flow characteristics using a surfactant solution in a spiral pipe. In his experiment it is revealed that the particles floating in the channel was distributed evenly along the pipe caused by the axial velocity and tangential velocity. Both types of the velocities in turbulent flow caused surfactant particles oscillated.

Friction factor of Newtonian fluid increased along with the increasing Reynolds number. Unlike the non-Newtonian fluid, higher Reynolds number in pseudoplastic type decreases the friction factor up to a certain value. The increase in drag reduction is influenced by various factors such as the concentration ratio of the working fluid and additives as well as the temperature [5-7].

Investigation the drag reduction in spiral pipe has been conducted, i.e. Flow in a spiral pipe 1st and 2nd reports [8-9], the addition of biopolymers guar gum using various pipe ratio of P/D_i [10], addition of biopolymer CMC to crude oil flow suspension [11], Drag Reduction effect of fly ash slurries in spiral pipes [12], mud slurries characteristics in spiral pipes [13], and

silica slurries in spiral pipes [14]. The new geometry of spiral pipe using pentagonal cross section and nanofluid as working fluid has also been researched lately by Yanuar *et al.* [15]. In these studies found that the effect of drag reduction is not only influenced by the amount of additives but also influenced by working fluid and geometry of the spiral pipe.

2.0 METHODOLOGY

2.1 Experimental Set-up

The coal sample and the experimental set up is shown in Figure 1 and 2, respectively. The coal slurries were circulated by pumping from tank 2 to tank 1. Compressor was used to keep the flow steady. Agitator used to keep homogeneous solution. Pitot tube used to measure velocity distribution along three cross sectional axis, and obtained five non-dimensional axial velocity data along each axis [16]. The three cross sectional axis of the spiral pipe can be seen in Figure 3. The length of flow measurement was 1550 mm using pressure transducer connected to DAQ and computer. Entrance length was 3000 mm to ensure the fully developed flow. The shear stress and shear rate could be obtained by measuring pressure drop gradient and velocity gradient, respectively. Weight concentration (C_w) in the mixture of coal slurries was varied by 30%, 40%, and 50%. The temperature measurement was kept in 27^o C. The density of coal is $1,5 \times 10^3$ (kg/m³) and particles diameter range between 1 – 50 mm. The homogeneity percentage of the coal was measured by comparing the coal mixed which was transported and coal deposition in the pipe. The average velocity of tested spiral pipe was calculated from the measured cross sectional area. CFD of flow visualization and velocity distribution used to validate experimental results.

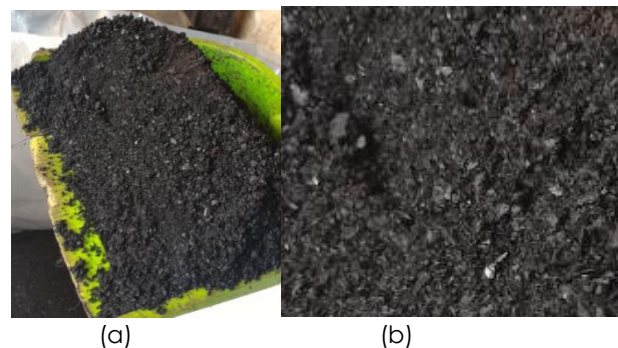


Figure 1 (a) Coal sample used in experimental, (b) Close up view of Coal ores

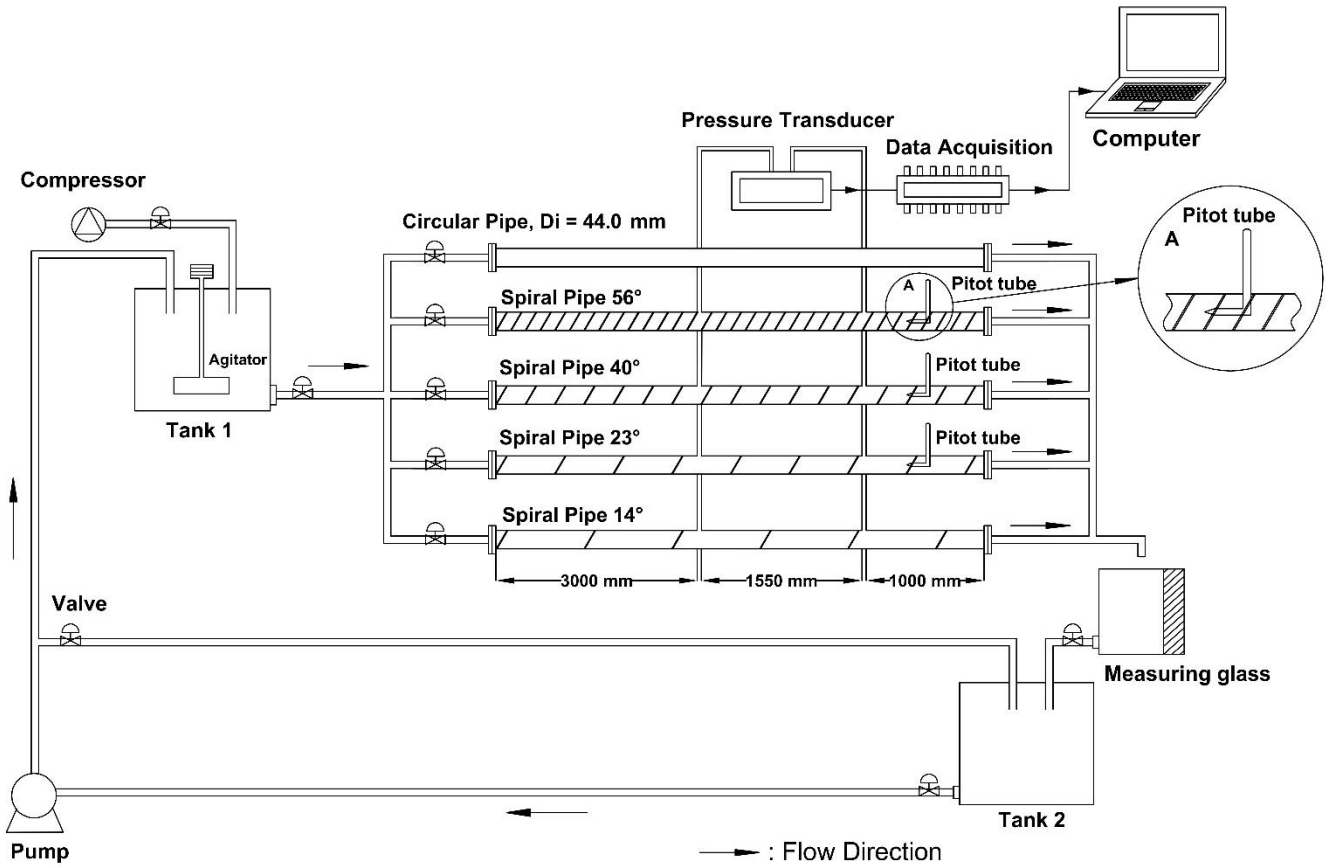


Figure 2 Experimental set up

The tested pipes is shown in Table 1. Circular pipe used as comparison pipe to investigate the flow characteristic in spiral pipes. Spiral pipes design and geometry differentiated by varying twisted angles.

Twisted angle was measured from horizontal axis. Diameter equivalent of spiral pipes was used in formula calculation.

Table 1 Tested Pipes

Pipes	D_i (mm)	D_o (mm)	D_e (mm)	Δd (mm)	P (mm)	P/D_o	β (°)
Circ.	44.0	44.0	44.0	-	-	-	-
S.P.I	33.6	43.0	38.0	4.5	512	11.9	14
S.P.II	33.8	44.4	37.0	5.3	311	7.0	23
S.P.III	34.5	44.5	36.8	5.0	156	3.5	40
S.P.IV	35.0	44.8	36.3	4.8	90	2.0	56

Figure 3, and 4 describe the geometry design of spiral pipe. The groove depth (Δd) defines the difference of maximum inner diameter (D_o) and minimum inner diameter (D_i). Helical twisting design based on the horizontal axis angle and the ratio of P/D_o . The increasing ratio of P/D_o make decreasing of pipe angle. In this research used four kinds of tested spiral pipes.

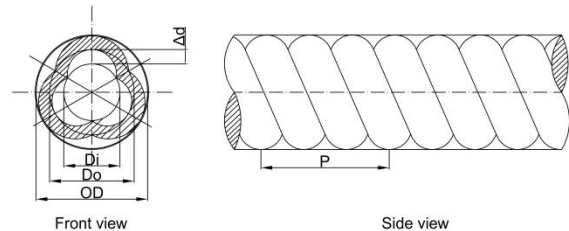


Figure 3 Sketch of spiral pipe

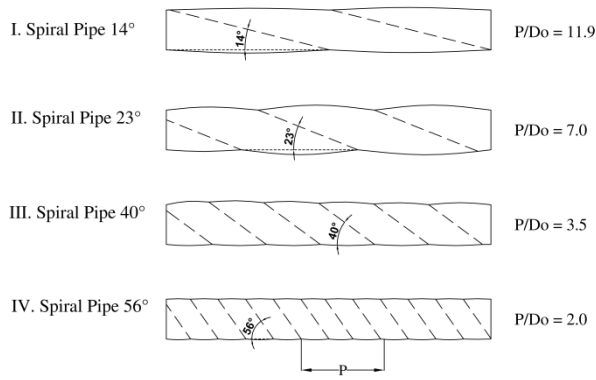


Figure 4 Angle and ratio design of spiral pipes

2.2 Geometry of Spiral Pipe

The difficult measurement of spiral pipe profile approached by calculate constant factor to find new equivalent radius of circular form. The method to approach cross sectional profile could be used elliptical form [17]. In this research was proposed to use equivalent circular form.

The area and perimeter of N in circular will best fitted with area of M in spiral by constant 0.70 as shown in Figure 5 (a) and (b).

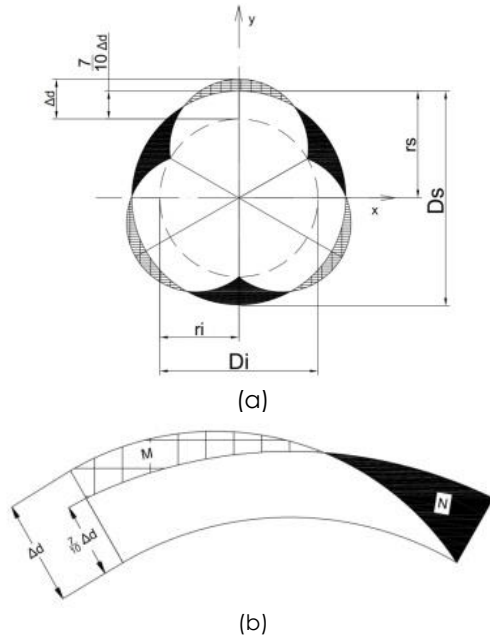


Figure 5 (a) Approachment spiral and circular form, (b) Comparison area and perimeter between spiral and circular form within sixth part

The relation among inner radius (r_i), groove depth (Δd), and radius of new circular approachment (r_s) with the constant factor described as follows :

$$r_s = r_i + \frac{7}{10} \Delta d \tag{1}$$

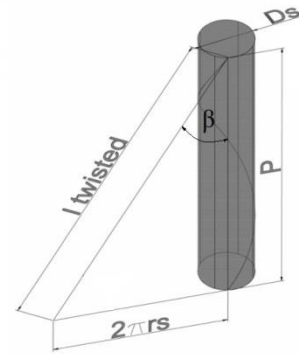


Figure 6 Relation among pitch, twisted length, radius, and twisted angle

$$l_{twisted} = \sqrt{(2\pi r_s)^2 + (P)^2} \tag{2}$$

$$l_{twisted} = \frac{P}{\cos \beta} \tag{3}$$

Twisted length has been obtained per pitch length. Thus, the total length of fluid flowing along the distance Δx can be obtained as follows :

$$\frac{\Delta x}{P} = \frac{l_{total}}{l_{twisted}} \tag{4}$$

From Equation (3) can be obtained total length (l_{total}) as follows :

$$l_{total} = \frac{\Delta x}{\cos \beta} \tag{5}$$

2.3 Rheology Model

Fluid characteristic obtained from experimental data is plotted in the moody chart. Laminar region refer to Hagen-Poiseuille line and turbulent region refer to Prandtl-Karman line.

Power law model used in non-Newtonian fluid model with the relation between shear stress (τ) and shear rate (γ) is proportional as follows :

$$\tau = K \left(-\frac{du}{dy} \right)^n = K (\gamma)^n \tag{6}$$

Where τ is shear stress, K and n is constant for the particular fluid, relationship change due to shear strain of non-Newtonian fluid. for $n = 1$ is for Newtonian behavior and $K = \mu$ become viscosity of Newtonian fluid.

Re' is the Generalized Reynolds Number for non-Newtonian model and Newtonian model if $n = 1$ and $K = \mu$, can be obtained from equation:

$$Re' = \frac{8n^n \rho D_e^n u^{2-n}}{2^n (3n+1)^n K} \quad (7)$$

Relation between shear stress and shear rate obtained by measuring pressure drop and flow rate as follows:

$$\frac{D_e \Delta P}{4l_{total}} = \mu \frac{8u}{D_e} \quad (8)$$

Where D_e is pipe equivalent diameter, ΔP is pressure drop, l_{total} is total twisted pipe length, μ is fluid dynamic viscosity, and u is average velocity. Power law index (n) can be obtained as follows:

$$n = \frac{d \ln(D_e \Delta P / 4l_{total})}{d \ln(8u / D_e)} \quad (9)$$

Power law index (n) determined from the slope of a log-log plot of shear rate and shear stress. Weight concentration of solid material in the mixture can be obtained as follows:

$$C_w = \frac{C_v \rho_s}{C_v \rho_s (100 - C_v)} = \frac{C_v \rho_s}{\rho_m} \quad (10)$$

Where C_w , C_v are concentrations of solid in percent by weight and volume, respectively. ρ_s and ρ_m are density of the solid phase and mixture phase, respectively.

Friction factor can be obtained using Darcy Equation as follows:

$$\lambda = \frac{2Dg\Delta h}{l_{total} u^2} \quad (11)$$

Where, λ is friction factor, g is gravitation, and Δh is the different height of manometer between two measuring point. Drag reduction (DR) is calculated as follows:

$$DR = \left| \frac{\lambda_{(water)} - \lambda_{(suspension)}}{\lambda_{(water)}} \right| \times 100\% \quad (12)$$

3.0 RESULTS AND DISCUSSION

3.1 Flow Characteristic of Coal Slurries Mixture

Coal slurries mixture contain weight concentration of solid particles. The rheology behavior was measured in circular pipe. The temperature of mixture was kept at 27°C because the properties is temperature dependent. Figure 7 shows the flow curve of mixture in various weight concentration using Equation (4) and water data $n = 1$ for comparison as Newtonian fluid. Mixture with $C_w = 30\%$ seems to become non linear with Power law index (n) = 0.92, obtained using Equation (8-9). Higher concentration of solid particles $C_w = 40\%$ and 50% decrease the Power law index with value 0.91 and 0.90, respectively. The rheology of coal slurries is pseudoplastic and the relation between shear rate and shear stress refer to Equation (6). The degradation effect of mixture also important to be measured by friction loss measurement before and after the test.

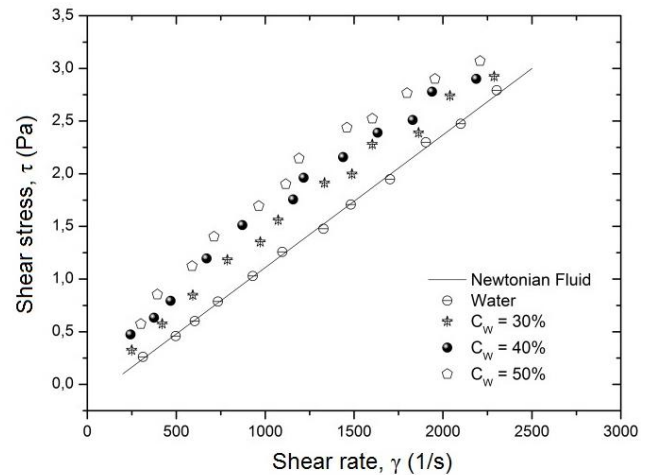


Figure 7 Flow curve of coal slurries

The viscosity behavior of the mixture also important to be investigated. The measurement using horizontal pipe viscometer for the $C_w = 30\%$, 40% and 50% were carried out and the results showed in Figure 8. The relation of shear rate and apparent viscosity of water is constant due to Newtonian fluid. Meanwhile, for coal slurries were changed decreasing by shear rate, and the apparent viscosity was used in calculation for Power law model. With the higher solid concentration decrease the Power law index and increase the viscosity of fluid. The effect of solid particles to change the flow behavior from Newtonian become non-Newtonian fluid depend on the concentration.

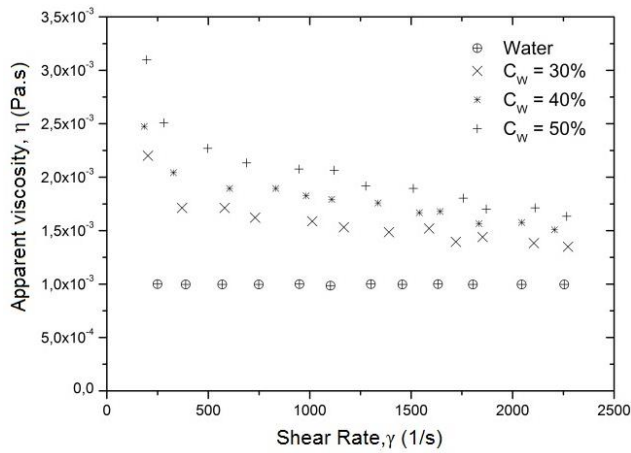


Figure 8 Apparent viscosity of coal slurries

3.2 Pressure Drop of Coal Slurries Flow

One of the parameter that can determine the flow performance of the coal slurries is wall friction factor using Moody chart. The effectiveness of using spiral pipe rather than circular pipe to transport fluid contain solid particles concentration will be considered according to friction characteristic and suspension homogeneity.

Figure 9 shows the use of circular pipe to carry coal slurries increased the friction factor significantly in low Re' , while in high Re' the friction factor tend to decreased. The effect of solid particles concentration to friction factor could not be

concluded due to the heterogeneous of solid particle that not dispersed uniformly.

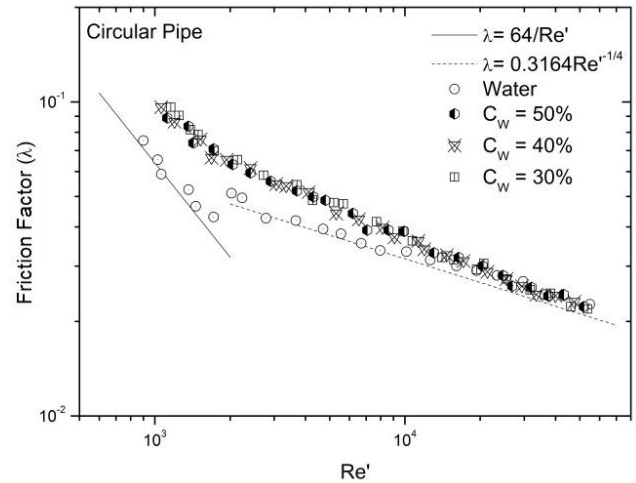


Figure 9 Friction factor of coal slurries in circular pipe

Friction factor in different angle of spiral pipe is shown in Figure 10. For $\beta = 56^\circ$, Friction factor for water is higher than in circular pipe, Figure 9, and for the mixture as well. On the other hand, the effect of swirling flow appeared, can be seen from the tendency of the increasing weight concentration lead decreasing the friction factor. Meanwhile, this spiral pipe ratio has not give better performance yet.

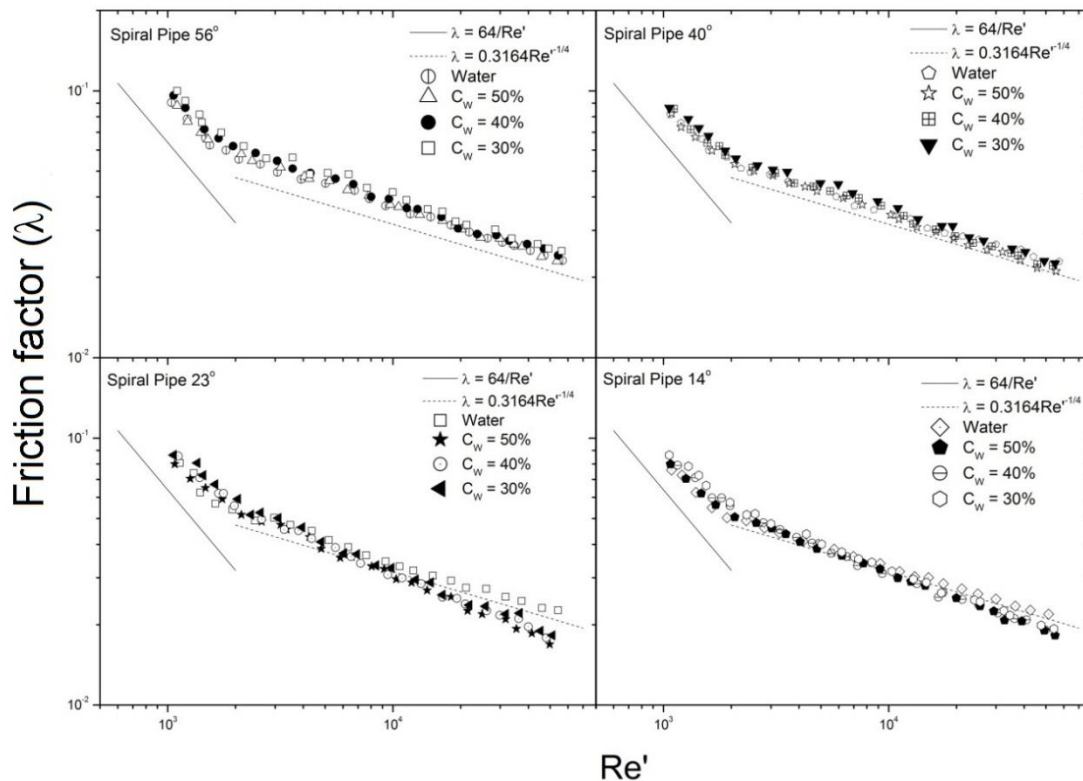


Figure 10 Friction factor of coal slurries in spiral pipe $\beta = 56^\circ, \beta = 40^\circ, \beta = 23^\circ, \beta = 14^\circ$

It needs to investigate the influence of decreasing twisted angle to friction factor. For spiral pipe with $\beta = 40^\circ$ friction factor tend to decreased compared to $\beta = 56^\circ$.

For $\beta = 23^\circ$ gives favorable result for friction factor. In high Re' ($Re' > 5 \times 10^3$) which is the optimum operational of spiral pipe utilization to transport solid particles show lower friction factor than those compare to water datas.

Spiral pipe $\beta = 14^\circ$ is the smallest twisted angle used in this experiment. Smaller angle decreases swirling flow effect. Friction factor for this design ratio tend to slightly increased compared to $\beta = 23^\circ$.

Spiral pipe $\beta = 23^\circ$ with ratio $P/D_o = 7.0$ give the best performance to transport coal slurries compared to the other tested pipes. Decreasing twisted angle of spiral pipe bring back the characteristic close to straight pipe.

3.3 Drag Reduction

Drag reduction shows the decreasing of coal slurries friction factor to water friction factor. It represents the efficiency in power requirement to transport the suspension fluids. Figure 11 shows Drag Reduction spiral pipes $\beta = 23^\circ$ and $\beta = 14^\circ$. Spiral pipe $\beta = 23^\circ$ give the highest DR around 30% for $C_w = 50\%$, Re' around 5.0×10^4 , while $\beta = 14^\circ$ reached the highest DR around 23% for $C_w = 50\%$, Re' around 5.5×10^4 .

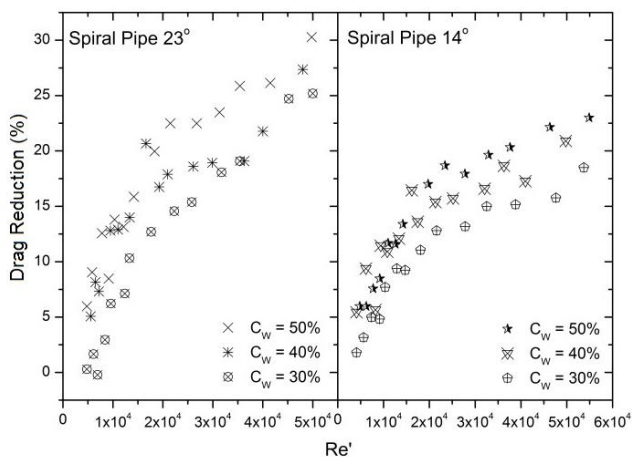


Figure 11 Drag reduction in spiral pipe $\beta = 23^\circ$ and $\beta = 14^\circ$

3.4 Homogeneity of Coal Slurries

Coal slurries are heterogeneous flow with high settling velocity, and solid particles are not dispersed uniformly.

Considering the homogeneity is important to see the effectiveness of transporting solid particles through test pipes. Figure 12 shows the homogeneity in whole test pipes for $C_w = 50\%$. At the same velocity spiral pipes shows the clear effectiveness in carrying solid particles with the range around 83-96% and circular pipe around 60-74% in velocity 0.2-1.5 m/s.

The higher velocity shows the higher homogeneity percentage. Spiral pipe $\beta = 40^\circ$ shows the least effective, while $\beta = 23^\circ$ shows the most effective with maximum homogeneity 96% at 1.5 m/s. From the results can be concluded that homogeneity was influenced by twisted angle, ratio P/D_o , and groove depth (Δd) takes a part as well.

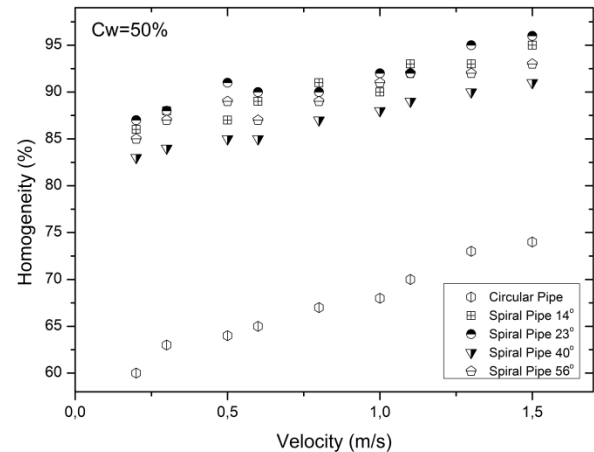
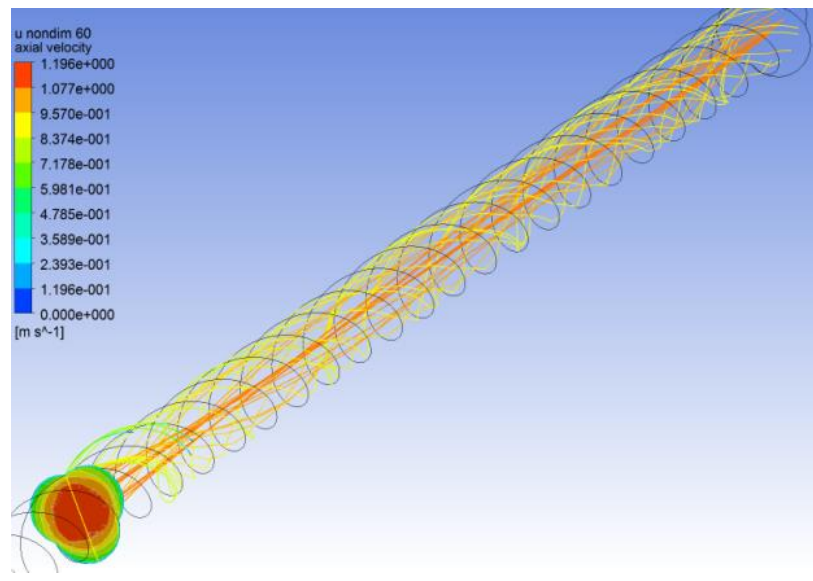
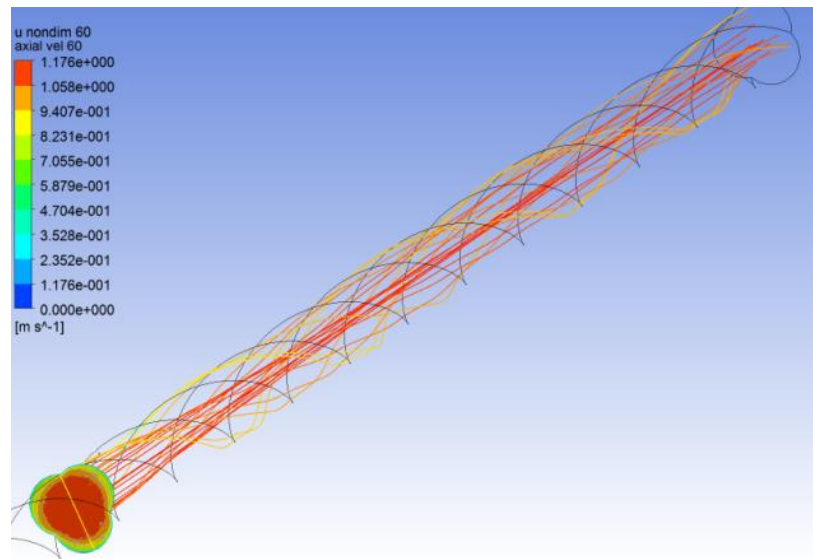


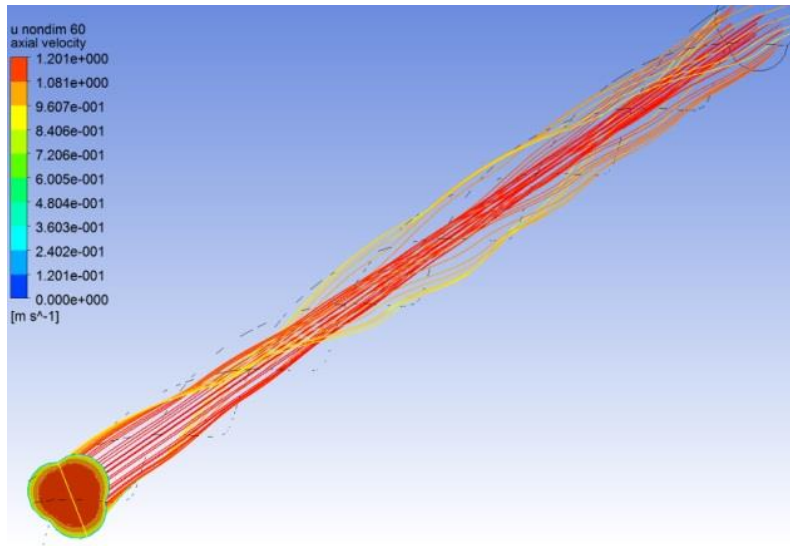
Figure 12 Coal slurries suspension homogeneity in test pipes

3.5 Flow Visualization and Velocity Distribution

It is important to investigate flow visualization in different spiral pipe angles. The numerical CFD simulation was carried out to make clear the flow pattern in spiral pipe influenced by twisted angle, pitch, and groove. The measurement of streamline velocity and velocity distribution in spiral pipe was conducted in cross sectional with non-dimensional distance $L/D_o = 60$, at $Re' = 5.0 \times 10^4$.

Figure 13 shows the comparison of streamline velocity for coal slurries flow among three different angles from one cross sectional axis. In high velocity turbulent region, because the wall groove, the wall roughness factor take into account. The wavy flow tend to occur along near wall region due to high velocity condition. The decreasing of angle or increasing of pitch reduce the mixing flow of suspension that can be seen from the thickness layer with red color. From the pressure drop results for fluid contain particles suspension like coal slurries, the effect of angle or pitch can be described for $\beta = 40^\circ$, with excessive mixing flow effect makes higher friction factor, thus, it become inefficient. Meanwhile, for $\beta = 14^\circ$, with pitch increase cause reduction in mixing flow affect the homogenous of coal slurries. Therefore, it is worthy to optimize in which ratio of spiral pipe give the most efficient flow.

(a). $\beta = 40^\circ$ (b). $\beta = 23^\circ$

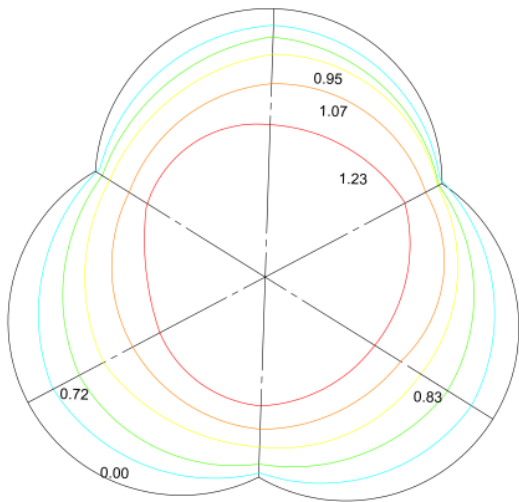


(c). $\beta = 14^\circ$

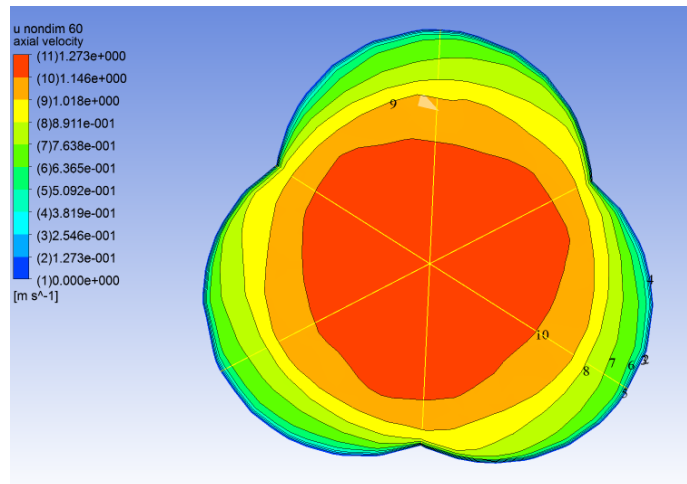
Figure 13 Flow pattern comparison of CFD results in different spiral pipe angle at $Re' = 5,0 \times 10^4$

The velocity distribution obtained from experimental then compared to numerical CFD simulation with the same parameter in boundary condition. Figure 14 shows the comparison for different cross sectional angle. The simulation results

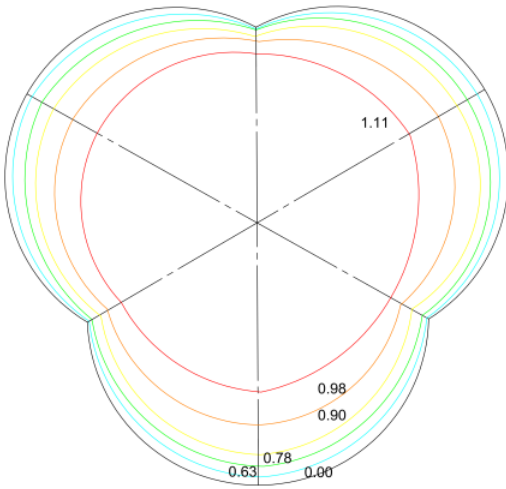
agree well with experimental, it can be seen from the profile pattern and non-dimensional axial velocity. The decreasing angle or increasing pitch affects the decreasing intensity in wavy flow and increasing thickness layer of flow parallel to the pipe axis.



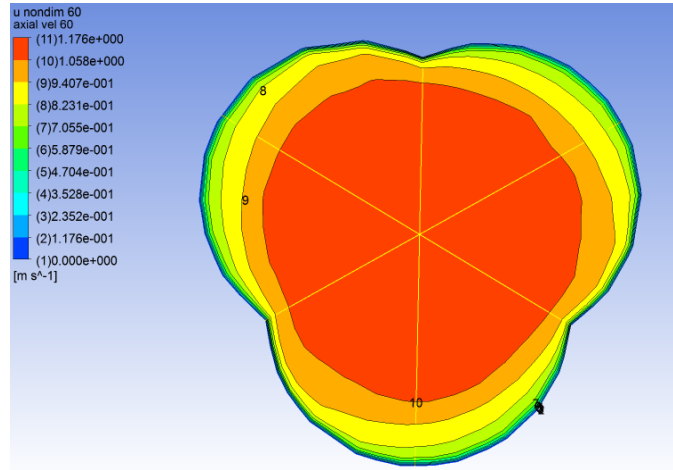
(a). $\beta = 40^\circ$ Experimental



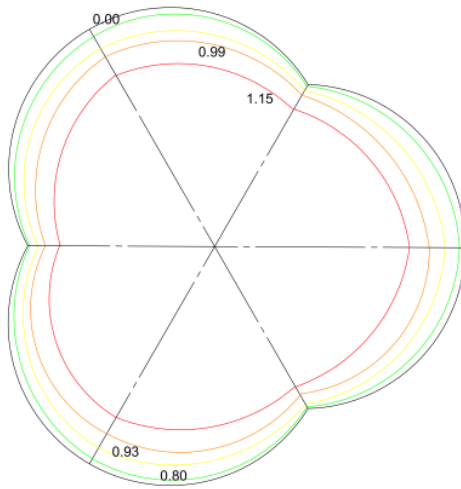
(d). $\beta = 40^\circ$ Numerical CFD Simulation



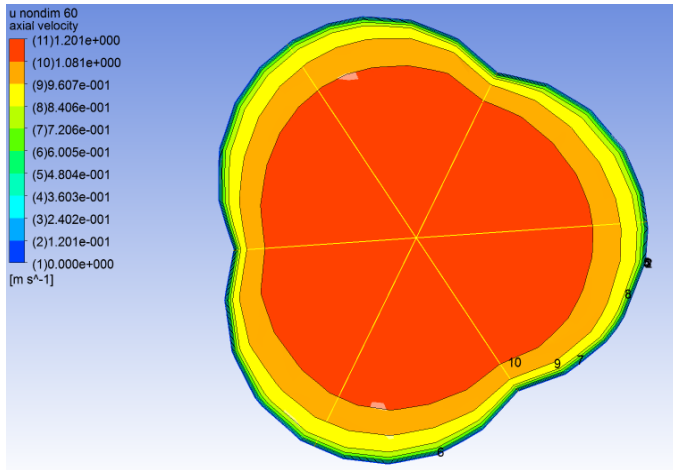
(b). $\beta = 23^\circ$ Experimental



(e). $\beta = 23^\circ$ Numerical CFD Simulation



(c). $\beta = 14^\circ$ Experimental



(f). $\beta = 14^\circ$ Numerical CFD Simulation

Figure 14 Velocity profile distribution comparison between CFD and experimental results in different spiral pipe angle, at $L/D_o = 60$, $Re' = 5.0 \times 10^4$

Non-dimensional axial velocity clearly described in Figure 15. Both results in experimental and simulation show that $\beta = 40^\circ$ more advance in near pipe axis region, yet, lower in near wall region due to the higher wavy flow intensity. On the other hand, the comparison between $\beta = 23^\circ$ and $\beta = 14^\circ$ are interesting, $\beta = 23^\circ$ tend to show the most efficient to carry coal slurries compared to other pipe angles. Velocity profiles and drag reduction of $\beta = 23^\circ$ slightly above $\beta = 14^\circ$, one of the cause is the effectiveness flow of particles suspension regarding to pipe angle that produces swirling flow and flow homogeneity. Thus, the optimum ratio of spiral pipe to carry coal slurries is $\beta = 23^\circ$, $P/D_o = 7.0$

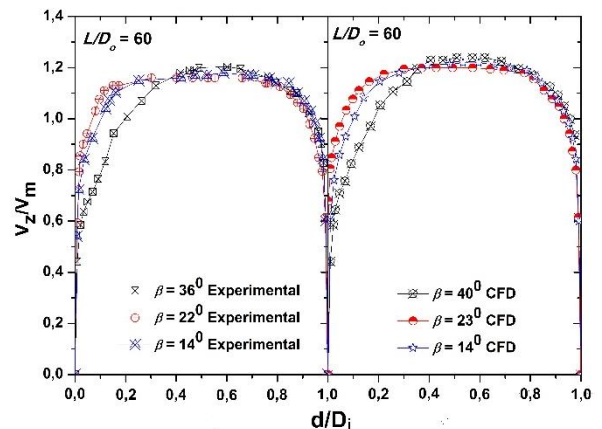


Figure 15 Velocity distribution comparison of experimental results at $L/D_o = 60$, $Re' = 5.0 \times 10^4$

4.0 CONCLUSION

From the friction factor point of view, higher angle shows the excessive swirling flow and increase the chaotic level, while smaller angle decreases swirling flow effect. Spiral pipe $\beta = 23^\circ$ with ratio $P/D_o = 7.0$ gives the optimum performance to transport coal slurries compared to other tested pipes due to the effectiveness flow of particles suspension regarding to pipe angle which produces swirling flow and mixed flow homogeneity.

Spiral pipe $\beta = 23^\circ$ give the highest DR trend in high Re' . At the same velocity, spiral pipes shows more effectiveness in carrying solid particles compared to circular pipe. With higher velocity causes higher homogeneity percentage. Spiral pipe $\beta = 40^\circ$ shows the least effective, while $\beta = 23^\circ$ shows the most effective with maximum homogeneity 96% at 1.5 m/s. It can be concluded that homogeneity was influenced by flow velocity, helical angle, ratio P/D_o , and groove depth (Δd).

Velocity streamline and distribution were obtained from numerical CFD simulation with non-dimensional parameters successfully validated experimental results.

Nomenclature

C_v	volume concentration, %
C_w	weight concentration, %
D_e	equivalent diameter based on the hydraulic mean depth, m
D_i	minimum inner diameter, m
D_o	maximum inner diameter, m
DR	Drag Reduction percentage, %
d/D_i	non-dimensional distance normal to pipe wall
K	consistency index in the power law fluids, Pa.s
l_{total}	total length of fluid flow, m
L/D_o	non-dimensional length distance
n	Power Law index, dimensionless
OD	outer diameter, m
P	pitch length, m
Re'	Generalized Reynolds Number, non-dimensional
u	average velocity, m/s
V_z/V_m	non-dimensional axial velocity to mean velocity
Δd	groove depth, m
β	twisted angle, $^\circ$
γ	velocity gradient/shear rate, (1/s)
λ	friction factor, dimensionless
ρ_s	density of solid phase, kg/m ³

ρ_m	density of mixture phase, kg/m ³
τ	shear stress, (Pa.s)

References

- [1] Baha, E. A. 2002. *Slurry System Handbook*. McGraw-Hill.
- [2] Leninger, D., Erdmann, W. and Kohling, R. 1978. Dewatering of Hydraulically Delivered Coal. Working paper E-7, BHRA Group, Hydrotransport 5, Hanover.
- [3] Yanuar, Gunawan, Sunaryo, A. Jamaluddin. 2012. Micro-bubble Drag Reduction on a High Speed Vessel Model. *Journal of Marine Science and Application*. 11(3): 301-304.
- [4] Munekata, M., Matsuzaki, K. and Ohba, H. 2006. Vortex Motion in a Swirling Flow of Surfactant Solution with Drag Reduction. *Journal of Fluids Engineering*. 128(1): 101-106.
- [5] Pouranfard, A. R., Mowla, D. and Esmaeilzadeh, F. 2014. An Experimental Study of Drag Reduction by Nanofluids through Horizontal Pipe Turbulent Flow of a Newtonian Liquid. *Journal of Industrial and Engineering Chemistry*. 20(2): 633-637.
- [6] Tamano, S., Ikarashi, H., Morinishi, Y. and Taga, K. 2015. Drag Reduction and Degradation of Nonionic Surfactant Solution with Organic Acid in Turbulent Pipe Flow. *Journal of Non-Newtonian Fluid Mechanics*. 215: 1-7.
- [7] Yang, S. Q. and Ding, D. 2013. Drag Reduction Induced by Polymer in Turbulent Pipe Flows. *Chemical Engineering Science*. 102: 200-208.
- [8] K. Watanabe, T. Maeda, T. Iwata, H. Kato, 1984. Flow in a spiral Tube, 1st Report, Velocity Distribution and Pressure Drop. *JSME*. 27(228).
- [9] K. Watanabe, T. Iwata, H. Kato. 1984. Flow in a Spiral Pipe, 2nd Report, Hydraulic Transport of Solids in a Horizontal Pipe. *JSME*. 27(230).
- [10] Yanuar, Gunawan. and Baqi, M. 2012. Characteristics of Drag Reduction by Guar Gum in Spiral Pipes. *Jurnal Teknologi (Sciences & Engineering)*. 58: 95-99.
- [11] Yanuar, Waskito, K. T., Gunawan, Budiarto. 2015. Drag Reduction and Velocity Profiles Distribution of Crude Oil Flow in Spiral Pipes. *International Review of Mechanical Engineering*. 9(1): 1-10.
- [12] Watanabe, K., Kamoshida, T. and Kato, H. 1988. Drag Reduction on Fly Ash Slurries in a Spiral Tube. In Proceeding of 1st World Conference on Experimental Heat Transfer, Fluid Mechanics and Thermodynamics. 693-699.
- [13] Yanuar, Ridwan, Budiarto, Koestoer, R. A. 2009. *Hydraulics Conveyances of Mud Slurry by a Spiral Pipe*. *Journal of Mechanical Science and Technology*. 23: 918-922.
- [14] Yanuar, Gunawan, and Sapiah, D. 2015. Characteristic of Silica Slurry Flow in a Spiral Pipe. *International Journal of Technology*. 6: 916-923.
- [15] Yanuar, Mau, S., Waskito, K. T., Putra, O.A. and Hanif, R. 2017. Drag Reduction of Alumina Nanofluid in Spiral Pipe with Turbulent Flow Conditions. *AIP Conference Proceedings*. AIP Publishing. 1826(1): 020021.
- [16] H. Shibanuma, H. Kato, K. Watanabe, M. Fukushima. 1982. The Characteristics of Pitot Tubes in Dilute Polymer Solutions. *JSME*. 25(205).
- [17] Mizushima, T., Mitsuishi, N., and Nakamura, R. 1964. On the Flow of Power Model Fluid in Elliptic Tube. *Transaction of the Society of Chemical Engineering Japan*. 28(8): 648-652.